Published in final edited form as:

Otol Neurotol. 2017 April ; 38(4): 577–584. doi:10.1097/MAO.0000000000001330.

Middle-Ear Sound Transmission Under Normal, Damaged, Repaired and Reconstructed Conditions

Wei Dong, PhD[1,2], **Ying Tian, MD**[2,3], **Xin Gao, MS**[1], and **Timothy T.K. Jung, MD**[1,2]

[1]Research Service, VA Loma Linda Healthcare System, Loma Linda, CA, 92374

[2]Department of Otolaryngology–Head and Neck Surgery, Loma Linda University Health, Loma Linda, CA, 92350

[3]Department of Otolaryngology, The First Affiliated Hospital, China Medical University, Shenyang, P. R. China, 110001

Abstract

Hypothesis—We hypothesize that current clinical treatment strategies for the disarticulated or eroded incus have the effect of combining the incus and stapes of the human middle ear (ME) into one rigid structure, which, while capable of adequately transmitting lower-frequency sounds, fails for higher frequencies.

Background—ME damage causes conductive hearing loss (CHL) and while great progress has been made in repairing or reconstructing damaged MEs, the outcomes are often far from ideal.

Methods—Temporal bones (TBs) from human cadavers, a laser Doppler vibrometer (LDV) and a fiber-optic based micro-pressure sensor were used to characterize ME transmission under various ME conditions: normal; with a disarticulated incus; repaired using medical glue; or reconstructed using a partial ossicular replacement prosthesis (PORP).

Results—Repairing the disarticulated incus using medical glue, or replacing the incus using a commercial PORP, provided similar restoration of ME function including almost perfect function at frequencies below 4 kHz, but with more than a 20-dB loss at higher frequencies. Associated phase responses under these conditions sometimes varied and seemed dependent on the degree of coupling of the PORP to the remaining ME structure. A new ME-prosthesis design may be required to allow the stapes to move in three-dimensional space to correct this deficiency at higher frequencies.

Conclusions—Fixation of the incus to the stapes or ossicular reconstruction using a PORP limited the efficiency of sound transmission at high frequencies.

Keywords

Human temporal bone; middle ear transmission; laser Doppler vibrometer; fiber-optic pressure sensor; repaired ossicular chain; partial ossicular replacement prosthesis; middle ear pressure gain; middle ear transfer function

Dr. Wei Dong, VA Loma Linda Healthcare System, Research Service (151), 11201 Benton Street, Loma Linda, CA 92374, Phone: 909-825-7084x2899, Fax: 909-796-4508, Wei.Dong@va.gov.

Background

The middle ear (ME) is a small, complex three-dimensional (3D) mechanical system that collects energy from sound waves in the external ear canal, and passes this vibratory signal to the cochlea. The ME's fundamental function is to provide an impedance match between the ear canal and the fluid filled cochlea, which results in a pressure gain to the incoming signal (1). Recent studies demonstrate that sound-evoked vibrations of the tympanic membrane (TM) and ossicular chain, consisting of the malleus, incus and stapes, are complex and highly frequency-dependent. At low frequencies, the TM moves in a simple in-phase displacement pattern that precisely mimics the incoming acoustic signal, and the three ossicles move together as one 'rigid' body (2,3) in a simple rotational mode, about an anatomical axis defined by a line passing through the anterior process of the malleus and the short process of the incus (1). With increasing frequency, the TM and ossicle motions become more complex in that the TM's vibration pattern breaks up into small zones that vibrate with different phases (4,5) and the ossicles lose their internal coherence and slippage occurs between them (6) as they exhibit rotations about axes that change in position during the vibratory cycle (7–12). In animal experiments (e.g., gerbil, cat), even deformation of the distal part of the malleus' manubrium that attaches to the TM is observed at high frequencies of the animal's hearing range (7,13). The stapes moves in 3D space with a linear piston-like movement at low frequencies and with additional rocking-like motions along the long and short axes of its footplate at higher frequencies (12,14,15). Understanding the complex motion of the ossicles and their corresponding importance to hearing is an ongoing area of ME research (14,16).

Any defect in the ME's conduction system results in a reduction in the initial drive to the cochlea and can cause a hearing loss of up to 60–70 dB (17). While significant progress has been made towards restoring hearing by repairing or reconstructing the ossicular chain using either a partial or a total ossicular replacement prosthesis (PORP or TORP, respectively), the postoperative outcome varies and hearing is often far from ideal (18–20). To ideally restore hearing and optimize surgical approaches, a quantitative understanding of the performance of the repaired or reconstructed ME is required.

The current study focuses on advancing our understanding of the remaining conductive hearing loss (CHL) following surgical treatments aimed at repairing the incus and stapes with medical glue or reconstructing the ossicular chain using a PORP in human temporal bones (TB). ME transmission was characterized under both normal and pathological conditions by measuring both velocity at various points along the ossicular chain and pressures at the input and output of the ME system, i.e., at the TM close to the umbo and in scala vestibuli (SV) just behind the stapes, respectively. Our results suggest that while these treatments restored normal ME function at low frequencies, i.e., those <4 kHz, they failed to restore function at higher frequencies, where complex 3D motion along the ossicular chain may be important.

Methods

Acoustic stimulation and data acquisition

Pure-tone stimuli from 200–20,000 Hz at 80 to 100 dB sound pressure level (SPLs in decibels re 20 μPa p-p) were digitally generated with a sampling frequency of 200 kHz using a commercial system [Tucker-Davis Technologies (TDT System III)] and delivered by a Fostex speaker. Stimulus-generation and data-acquisition software was written in Matlab (Mathworks, Natick, MA) and TDT's Visual Design Studio (Tucker-Davis).

Temporal bone preparation

The study protocol was approved by the Institutional Review Board of the VA Loma Linda Healthcare System. The TB preparation and surgical approaches were similar to a previously published study (21) and are summarized here. Eleven human TBs contributed to the current study, and were removed from commercially available cadavers by a board-certified otologist (TTKJ) using the intracranial Schuknecht method (22) and frozen in saline (−20°C) immediately. Then, each TB was defrosted in a 4°C refrigerator overnight before the experimental day. The ME was visually checked for damage by the otologist using an operating microscope. The bony wall of the ear canal was shortened to a length of about 0.5–1 cm. Then, a 3-mm diameter opening was made in the anterior wall of the ear canal and covered by a clear-glass window sealed with high vacuum grease (Dow Corning Corp) to allow the laser Doppler vibrometer (LDV, OFV-5000, Polytec) to be focused on the umbo in the direction of the stapes' piston-like motion (23). The facial recess was opened for access to the middle and inner ear, and the stapedial tendon was severed to improve access to the area surrounding the footplate of the stapes. The TB was fixed with dental cement on a holder with a flexible joint allowing rotation of the preparation. In addition, the holder was positioned on a motor controlled XYZ stage that could move in 1 μm steps in 3D space and rotate ± 10° in two directions. After initial measurements of velocity responses along the ossicular chain, a 200–300 μm in diameter hole was made in the wall of the SV next to the stapes in order to introduce the micro-pressure sensor. The velocity phase at the round window membrane and stapes was measured before and after drilling the SV hole and introducing the micro-pressure sensor. A half-cycle difference between the two measurements verified the absence of air bubbles that might have been introduced during the freezing/thawing process or by the micro-pressure-sensor insertion. Preparations with abnormal phase relationships were excluded in data presentation. Saline was regularly sprayed onto the TB preparation to prevent changes to the ME measures due to the TB drying out.

Micro-pressure sensor

The design, construction, and calibration of the fiberoptic micro-pressure sensor has been described previously (24,25). The sensors used in the present study were 125 μm in outer diameter (26) and were calibrated individually in air before and after the measurements by comparing pressure responses to sound stimuli from 0.2 to 70 kHz measured by a well-calibrated ultasound Sokolich probe tube microphone. The sensors operate linearly with a sensitivity of approximately −60 dB V for an 80 dB SPL stimuli and were flat to within a few decibels to at least 50 kHz.

Experimental design

As shown in Fig. 1A, ME transmission was characterized by simultaneously measuring velocity responses of the stapes (V_{stapes}), pressure responses at the TM close to the umbo (P_{TM}) and in SV next to the stapes (P_{stapes}) using LDV, a Sokolich probe tube microphone and a micro-pressure sensor, respectively, under both normal and pathological conditions, which included disarticulated incus and stapes, repair by either fixing the incus and stapes with medical glue or reconstruction of the ossicular chain with a PORP. The PORPs (ALTO Offset Titanium Partial Porthesis, P/N-650, Grace Medical) and medical glue (Otomimix Calcium Phoshate Bone Void Filler, Gyrus Acmi) used are commonly utilized in otologic surgical practice. The tip of the Sokolich probe-tube microphone was visually positioned as close as possible to the umbo and the micro-pressure sensor was introduced into the SV close to the stapes (27). Due to the limited working space around the stapes and the requirement to simultaneously measure P_{stapes}, stapes velocity was measured at an angle of ~40°–60° relative to its piston-like motion direction, which was not corrected for because comparisons between normal and pathological conditions were performed within the same TB with the same approaches.

Data analysis

ME pressure gain (MEPG) and a local transfer function (LTF) of the ossicles were used to characterize ME transmission. MEPG is defined as the ratio of P_{stapes} to P_{TM} while LTF is defined as the ratio of $V_{ossicle}$ to P_{TM}. The group delay is defined as the negative slope of the phase-versus-frequency curve for either MEPG and LTF and was used to evaluate ME transmission times.

Controls

The fenestration for introducing the sensor into the SV was very close to the stapes footplate and sealing it with dental impression material (Jeltrade, L.D. Caulk Co.) was challenging and risked fixation of the footplate. Therefore, in eight out of eleven cases the hole was left open based on the results that (1) there was a maximum of ~4 dB difference at frequencies below 1.5 kHz in the average stapes LTF before and after the SV hole across 11 TBs (Fig. 1B) and (2) MEPGs were similar for SV hole open (gray) and sealed (black) in a representative experiment (Fig. 1C) and the average MEPG variation of three TBs after sealing the hole appeared to be within 2 dB of their pre-sealed values across test frequencies (black line in Fig. 1D). In addition, the effects of preparation vibration was also demonstrated using average velocity responses from a random location on the TB, which were far less than stapes responses at frequencies below ~14 kHz but were similar at higher frequencies (dashed-gray in Fig. 1B).

RESULTS

Data from all eleven TBs contributed to the initial normal control LTF findings summarized in Fig. 1B while a subset of 8 TBs for which a half-cycle phase difference was present between the velocity responses of the stapes and the round window membrane and for which the micro-pressure-sensor stayed intact and stable throughout the experiment were used for the results summarized below. Responses under normal control conditions were taken as the

baseline measure for each TB, against which variations under various pathological conditions were referenced.

1. Middle-ear pressure gain under normal condition

Figure 2 illustrates the characteristics of MEPG under normal conditions. On average MEPG across eight TBs, peaked at 1 kHz, and then gradually decreased to result in a value of ~10 ± 5 dB up to about 12 kHz (black line in Fig. 2A). The average phase between 2–16 kHz appeared to vary linearly with frequency (black in Fig. 2B) and suggested a group delay of ~75 μs calculated along a linear fit (thin line in Fig. 2B). Our results were consistent with published fresh TB data using similar surgical approaches to obtain MEPG measurements, but using a larger size micro-pressure sensor, 167 μm OD, with the SV hole sealed completely after sensor introduction [gray lines in Fig. 2 and (21)]. While the Nakajima phase data indicate a slightly longer group delay (steeper slope) this was likely due to the closer placement of the microphone probe tube to the umbo in the current study. These normal measures formed the baseline for the subsequent evaluation of ME sound transmission under pathological conditions.

2. Middle-ear transmission under pathological conditions

To characterize ME transmission under pathological conditions, both the stapes LTF and MEPG magnitude, phase and variation re: normal were plotted as a function of frequency for an individual TB (#25) in Fig. 3. Compared to ME transmission under normal control conditions (thick gray in Figs. 3A–B), disarticulation of the incus and stapes caused a 40 to 60-dB loss at frequencies below ~10 kHz as evaluated by both LTF and MEPG measures (thin dotted in Figs. 3A–D). The smaller loss at higher frequencies for this condition might be contaminated by the vibration of the preparation as shown in Fig. 1B. Repairing the incus and stapes with medical glue restored stapes LTF and MEPG almost completely at frequencies below 2 kHz, but the corresponding higher frequency results appeared far from the normal, i.e., ~20 dB loss at 8 kHz (thin gray in Figs. 3A–D). In addition, under the repaired condition, the MEPG phase-vs-frequency curve appeared steeper than normal which suggested a longer transmission time (thin gray in Fig. 3F).

Reconstructing the ossicular chain using a PORP resulted in similar restoration outcomes. The PORP was connected to umbo and stapes as shown in the leftmost panel in Fig. 3. Initially the prosthesis was positioned at an angle of about 20–30° to the stapes' piston-like motion (leftmost panel and thin dashed in Fig. 3). Under this condition the stapes LTF was similar to normal at frequencies below 2 kHz, and was ~20 dB smaller at higher frequencies (thin dashed in Fig 3C). When evaluated using MEPG, the loss was ~20 dB at frequencies below 3 kHz and ~40 dB at higher frequencies (thin dashed in Fig. 3D). The phase-versus-frequency curves appeared to be not as smooth as in normal conditions (thin dashed in Figs. 3E and F).

Adjusting the angle of the PORP to align with the stapes' piston-like motion direction appeared to provide better restoration of ME output than the angled case (thick dashed in Fig. 3). The stapes LTF was similar to that measured under the normal condition except for a notch at ~5 kHz (thick dashed in Figs. 3A and C). The MEPG showed ~20 dB loss across

the frequency range (thick dashed in Figs. 3B and D). In addition, the phase-versus-frequency curves of the stapes LTF and MEPG appeared to similar to the normal (thick dashed vs. gray in Figs. 3E and F), suggesting the ME transmission time was close to normal. Aligning the PORP along the piston-like motion direction appeared to improve the ME function above ~4 kHz. It is worth mentioning that in order to perform this adjustment, the PORP end connecting to the head of the stapes had to be enlarged, which resulted in it not being firmly connected to the head of the stapes. This loose connection might allow for more flexibility for the stapes to move in 3D space.

Figure 4 illustrates another example (TB #34) of ME function under pathological conditions. Compared to normal conditions (thick gray in Figs. 4A and B), disarticulating the incus and stapes produced a 40- to 60-dB loss in stapes LTF and MEPG (thin dotted in Figs. 4A–D). Repairing the incus and stapes using medical glue restored transmission below 1 kHz, however, the loss at higher frequencies was still notable, ~40 dB maximum (thin gray in Figs. 4A–D), and the transmission group delay appeared to be longer (thin gray in Figs. 4E and 4F). The incus was then replaced with a PORP, which was aligned with the piston-like motion direction of the stapes with the PORP head connecting to the manubrium (leftmost panel of Fig. 4). Performing a PORP replacement improved transmission by at least 40 dB at frequencies below 4 kHz (within 10 dB of normal), but left a difference of ~20-dB from the normal control condition at higher frequencies (black dashed in Figs. 4A–D). While the group delays under PORP conditions were similar to those under normal condition, the stapes LTF and MEPG phase-vs-frequency response showed about a 0.5-cycle shift at most frequencies (see double arrow in Figs. 4E and F), which is explained below.

Figure 5 illustrates the coupling of the PORP to the remaining ME structures using comparison of velocity phase responses measured at adjacent locations, i.e., at the PORP-head vs. the umbo, or at the PORP-shoe vs. the stapes (white dots in the left panel), for the two TBs shown above. If the phase difference lines up with zero or one cycle, it suggests that the two locations moved together as one rigid body. For TB #25 (refer to Fig. 3), the PORP-head seemed to move together with the umbo at most of the frequencies, except at 6 to 11 kHz (black line in Fig. 5A). The PORP-shoe moved in-phase with the stapes at frequencies below 2 kHz and above 7 kHz, and led the stapes from 2 to 7 kHz. The phase variations at both ends of the PORP suggested that at those frequencies the PORP did not move with the attaching structure as a rigid body, and was probably influenced by motion along other directions because the PORP-shoe was not firmly attached to the stapes. This explains the phases of stapes LTF and the MEPG in Figs. 3E and F. For TB #34, the PORP-shoe moved together with the stapes at all frequencies (gray in Fig. 5B) indicating a firm attachment, however, a 0.5-cycle difference developed between the umbo and the PORP-head at frequencies above 2 kHz (gray in Fig. 5A and recording locations in the left panel), which might suggest there was a kind of lever-motion occurring between the edge of the PORP-head relative to its center. The other points along the PORP worked as one rigid body (not shown), thus this 0.5-cycle difference seemed to account for the 0.5-cycle difference in the stapes LTF and MEPG presented in Figs. 4E and F.

Figure 6 summarizes ME transmission under pathological conditions evaluated by average stapes LTF (Fig. 6A), and average MEPG (Fig. 6B) across eight TBs. Repairing the incus

and stapes using medical glue restored ME transmission at frequencies below 4 kHz to within 10 dB on average, but was less effective at higher frequencies, leaving an ~20 dB loss (solid lines in Fig. 6A and 6B). Results of PORP reconstruction were ~5 dB worse than the repaired condition at frequencies below 1 kHz but provided similar results at other frequencies (dashed lines in Fig. 6A and 6B).

Discussion

The current study focused on characterizing ME transmission, under both normal control and pathological conditions. ME transmission was characterized by stapes LTF and MEPG with direct measurements of V_{stapes}, P_{TM} and P_{stapes}. The manually induced pathological conditions allowed us to quantify ME transmission under disarticulated incus and stapes, repaired incus using medical glue and replaced incus using a commercial PORP conditions. ME transmission may vary for different TB conditions, e.g., cochlear input impedance has been found to be different for defrosted versus fresh TBs (28) and the main factor appeared to be air in the defrosted preparations. Air contamination was checked for in the current study by verifying a 0.5-cycle phase difference between the stapes and the round window membrane. In addition, the tendon of stapes had to be cut because of the simultaneous measurements of V_{stapes} and P_{stapes} which may have some effect on the stability of the stapes. The SV hole for introducing the micro-pressure senor was left open in most preparations. However, the MEPG was found to be similar to published results using fresh TBs with the SV hole completely sealed [Fig. 2 and (21)] and variation upon leaving the SV hole unsealed in stapes LTFs and MEPGs was small (Fig. 1). To reiterate, the evaluations of the repair and reconstructed ossicular chain were achieved internally within the same TB under the same conditions. Thus, the results should be valid for demonstrating changes in ME transmission due to pathological conditions.

The normal human ME provides pressure gain for frequencies from 200 Hz to 20 kHz, which is more effective at the lower frequencies (Fig. 2). In the current study, MEPG was directly measured by comparing P_{stapes} to P_{TM}. P_{stapes} represented the output of ME pressure, which can also be considered as the dominant initial drive to the cochlea because the pressure at the round window side is close to zero, the atmospheric air pressure (21). Thus, P_{stapes} could be correlated with auditory brainstem response (ABR) results used clinically to evaluate the outcomes of ME repair or reconstruction.

Disarticulation of the incus from the stapes caused more than a 40-dB loss up to 14 kHz as evaluated by either stapes LTF or MEPG as illustrated in Figs. 3 and 4. The loss at higher frequencies was less, but this result might be contaminated by the vibration of the whole TB (Fig. 1B) even though the TB was glued to a holder using dental cement. This high frequency contamination may be lessened in future studies by positioning the TB on a cushion (based on verbal communication with HH Nakajima). Repairing the ossicles with surgical glue or reconstructing them using a PORP showed similar outcomes as illustrated in Figs. 3, 4 and 6, with restoration to within 5 to 10 dB at low frequencies (i.e., ≤~4 kHz) but left a loss of ~20 dB at the higher frequencies. In addition, the ME-transmission group delay did not always recover to baseline values measured under normal control conditions, which can be explained by the coupling of the PORP to remaining ME structures (Fig. 5). Our

results were consistent with clinical outcomes (18–20) and support PORP alignment along the stapes' piston motion direction (Fig. 3) and connection of the PORP to the umbo (Figs. 3, 4 and 5) so as to restore the transmission time.

The repair and reconstruction strategies used in the current study were designed to simulate those used in the clinic and resulted in a 'rigid' ossicular chain, which may limit complex motion along the ossicular chain, especially at the stapes. When the PORP was loosely coupled to the head of the stapes, the reconstruction of the ME transmission showed better restoration at high frequency regions (Fig. 3), consistent with the notion that the 3D motion of the stapes seems to be important for high frequency hearing (12,14,15). Thus, to ideally restore ME transmission, it may be necessary to develop an ossicular/PORP reconstruction device that mimics the normal 3D motion as closely as possible. The experimental design used in this study can be used to evaluate different or new ossicular prostheses designed to more accurately mimic complex ossicular chain motion.

Acknowledgments

The authors thank Barden B Stagner for his assistance in preparing the manuscript. The study was supported by the NIDCD (R01 DC011506) to WD, and the Research Fund of the Department of Otolaryngology–Head and Neck Surgery, Loma Linda University Health.

This study was supported by the NIDCD R01 (DC011506) to WD (NIH) and the Research Fund of the Department of Otolaryngology–Head and Neck Surgery, Loma Linda University Health.

References

1. Rosowski, JJ. Sensors and Sensing in Biology and Engineering. Barth, FG.Humphrey, JA., Secomb, TW., editors. Vol. XII. Springer; 2003. p. 59-69.
2. Wever, EG., Lawrence, M. Physiological acoustics. Princeton University Press; 1954.
3. Von Bekesy, G. Experiments in hearing. McGraw-Hill; 1960.
4. Rosowski JJ, et al. Computer-assisted time-averaged holograms of the motion of the surface of the mammalian tympanic membrane with sound stimuli of 0.4–25 kHz. Hear Res. 2009; 253:83–96. DOI: 10.1016/j.heares.2009.03.010 [PubMed: 19328841]
5. Tonndorf J, Khanna SM. Tympanic-membrane vibrations in human cadaver ears studied by time-averaged holography. J Acoust Soc Am. 1972; 52:1221–1233. [PubMed: 4638037]
6. Willi UB, Ferrazzini MA, Huber AM. The incudo-malleolar joint and sound transmission losses. Hear Res. 2002; 174:32–44. [PubMed: 12433394]
7. Decraemer WF, Khanna SM, Funnell WR. Malleus vibration mode changes with frequency. Hear Res. 1991; 54:305–318. [PubMed: 1938631]
8. Decraemer WF, Khanna SM, Funnell WR. A method for determining three-dimensional vibration in the ear. Hear Res. 1994; 77:19–37. [PubMed: 7928731]
9. Sim, JH., Puria, S., Steele, C. 3rd International Symposium on Middle Ear Mechanics in Research and Otology. World Scientific; p. 61-67.
10. Rosowski, JJ. Oxford Handbook of Suditory Science: The Ear. Fuchs, AP., editor. 2010.
11. Heiland KE, Goode RL, Asai M, Huber AM. A human temporal bone study of stapes footplate movement. Am J Otol. 1999; 20:81–86. [PubMed: 9918179]
12. Hato N, Stenfelt S, Goode RL. Three-dimensional stapes footplate motion in human temporal bones. Audiol Neurootol. 2003; 8:140–152. doi:69475. [PubMed: 12679625]
13. de La Rochefoucauld O, Olson ES. A sum of simple and complex motions on the eardrum and manubrium in gerbil. Hear Res. 2010; 263:9–15. DOI: 10.1016/j.heares.2009.10.014 [PubMed: 19878713]

14. Decraemer WF, et al. Scala vestibuli pressure and three-dimensional stapes velocity measured in direct succession in gerbil. J Acoust Soc Am. 2007; 121:2774–2791. [PubMed: 17550177]
15. Sim JH, et al. Complex stapes motions in human ears. J Assoc Res Otolaryngol. 2010; 11:329–341. DOI: 10.1007/s10162-010-0207-6 [PubMed: 20165895]
16. de la Rochefoucauld O, Decraemer WF, Khanna SM, Olson ES. Simultaneous measurements of ossicular velocity and intracochlear pressure leading to the cochlear input impedance in gerbil. J Assoc Res Otolaryngol. 2008; 9:161–177. DOI: 10.1007/s10162-008-0115-1 [PubMed: 18459001]
17. Merchant SN, et al. Analysis of middle ear mechanics and application to diseased and reconstructed ears. Am J Otol. 1997; 18:139–154. [PubMed: 9093668]
18. Merchant SN, Ravicz ME, Rosowski JJ. Mechanics of type IV tympanoplasty: experimental findings and surgical implications. The Annals of otology, rhinology, and laryngology. 1997; 106:49–60.
19. Meulemans J, Wuyts FL, Forton GE. Middle ear reconstruction using the titanium Kurz Variac partial ossicular replacement prosthesis: functional results. JAMA Otolaryngol Head Neck Surg. 2013; 139:1017–1025. DOI: 10.1001/jamaoto.2013.4751 [PubMed: 24135742]
20. Zaoui K, et al. Clinical investigation of flat panel CT following middle ear reconstruction: a study of 107 patients. Eur Radiol. 2014; 24:587–594. DOI: 10.1007/s00330-013-3068-7 [PubMed: 24275805]
21. Nakajima HH, et al. Differential intracochlear sound pressure measurements in normal human temporal bones. J Assoc Res Otolaryngol. 2008; 10:23–36. DOI: 10.1007/s10162-008-0150-y [PubMed: 19067078]
22. Nadol JB Jr. Techniques for human temporal bone removal: information for the scientific community. Otolaryngology–head and neck surgery: official journal of American Academy of Otolaryngology-Head and Neck Surgery. 1996; 115:298–305. [PubMed: 8861882]
23. Dong W, Decraemer WF, Olson ES. Reverse transmission along the ossicular chain in gerbil. J Assoc Res Otolaryngol. 2012; 13:447–459. DOI: 10.1007/s10162-012-0320-9 [PubMed: 22466074]
24. Olson ES. Observing middle and inner ear mechanics with novel intracochlear pressure sensors. J Acoust Soc Am. 1998; 103:3445–3463. [PubMed: 9637031]
25. Olson ES, Nakajima HH. Proc SPIE 9303.
26. Dong W, Olson ES. Supporting evidence for reverse cochlear traveling waves. J Acoust Soc Am. 2008; 123:222–240. DOI: 10.1121/1.2816566 [PubMed: 18177153]
27. Dong W, Olson ES. Middle ear forward and reverse transmission in gerbil. Journal of neurophysiology. 2006; 95:2951–2961. DOI: 10.1152/jn.01214.2005 [PubMed: 16481455]
28. Ravicz ME, Merchant SN, Rosowski JJ. Effect of freezing and thawing on stapes-cochlear input impedance in human temporal bones. Hear Res. 2000; 150:215–224. [PubMed: 11077205]

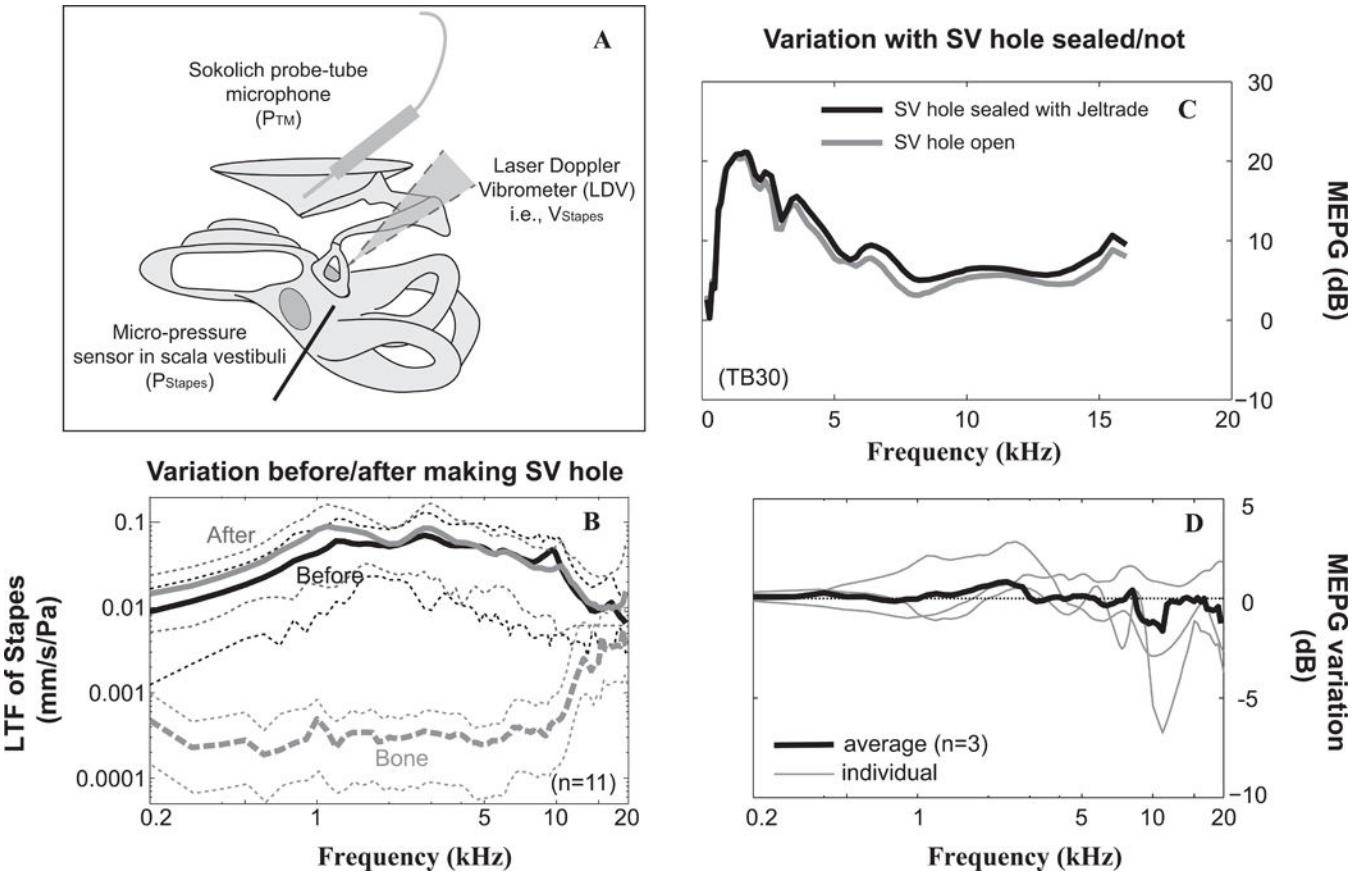

Figure 1. Experimental approach and control

A: Schematic of the experimental design for characterization of the ME system using a laser Doppler vibrometer, micro-pressure sensor and Sokolich probe-tube microphone. Velocity responses were measured along the ossicular chain, especially at the stapes while simultaneous pressure measurements were made at the tympanic membrane close to the umbo (P_{TM}) and in scala vestibule next to the stapes (P_{Stapes}). B: Effects of the SV hole on stapes LTF. Black and gray solid lines stand for average stapes LTFs across 11 TBs under the condition of cochlea intact and after the SV hole was made. Corresponding thin-dotted lines represent ±1 standard diaviation. In addition, averaged velocity responses from sourrounding bone normalized to P_{TM} together with ±1 standard diaviation were plotted as the gray dashed curve. C and D: effects of leaving SV hole unsealed on MEPG. C: Example from preparation of TB #30 demostrates MEPG under the condition of SV not sealed (solid gray line) or the SV fenestration sealed with Jeltrade (solid black line), respectively. D: MEPG variation upon slealing versus leaving the SV hole open. Thick line stands for average results across three individual TBs (thin lines). The maximum average variation of MEPG upon sealing the SV hole was ~2 dB. LTF: local transfer function; MEPG: middle ear pressure gain; P_{Stapes}: pressure in the SV next to the stapes; P_{TM}: pressure at the TM close to the umbo; SV: scala vestibule; TM: tympanic membrane.

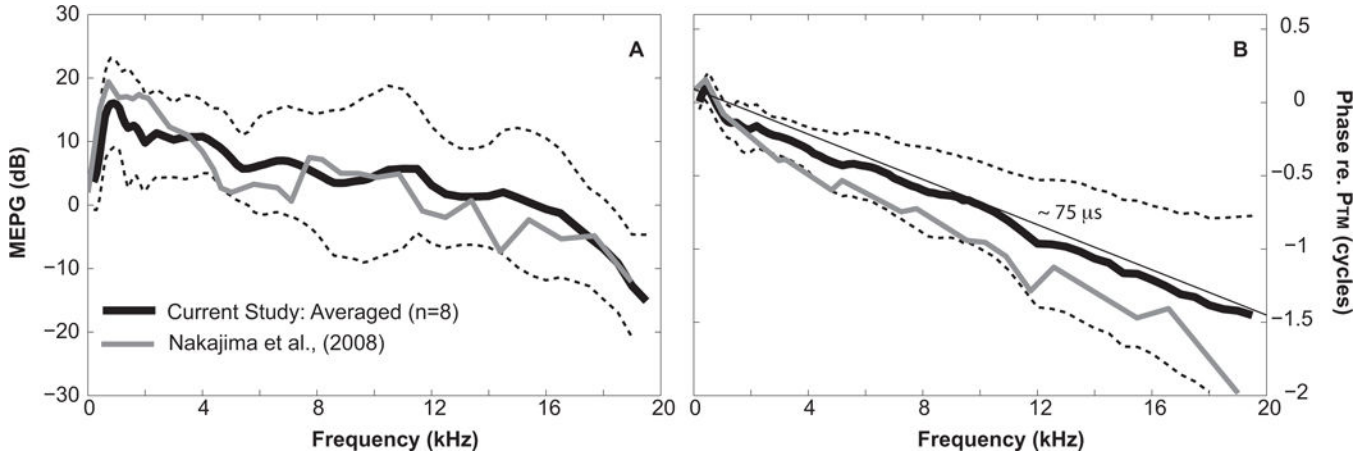

Figure 2. MEPG under normal control conditions

A: Amplitude of MEPG defined as P_{Stapes}/P_{TM} plotted in dB; B: phase of MEPG equals to P_{Stapes} referenced to P_{TM}. Black solid and dotted lines equal the average value across eight TBs ±1 standard deviation. Gray lines in both plots indicate published average results of six fresh TBs measured with 167 μm OD micro-pressure sensor, using similar surgical approaches with the SV hole sealed (Nakajima et al., 2008).

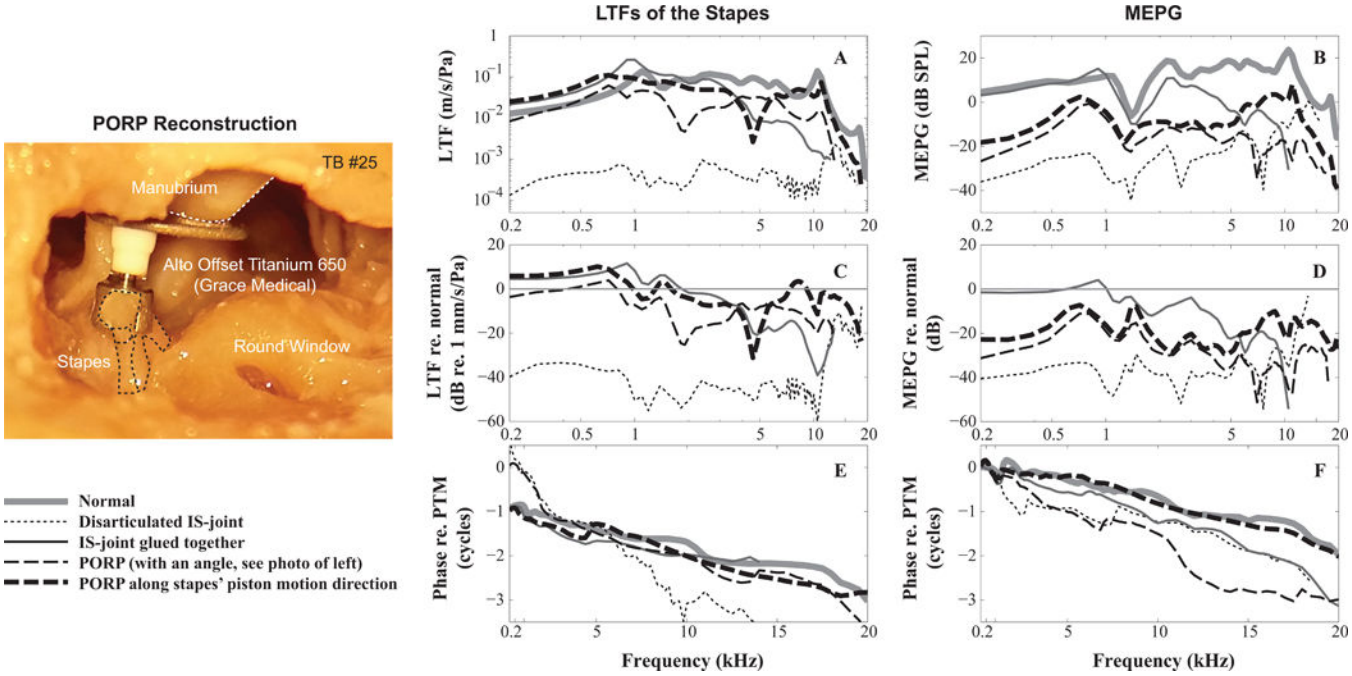

Figure 3. Stapes LTFs and MEPGs under normal and pathological conditions

A and B: amplitude of the stapes LTFs and MEPGs; (C and D) Variation of the stapes LTFs and MEPGs from normal condition; (E and F) phase of stapes LTFs and MEPGs. Figure legend at the bottom left. Micrograph panel at left side of figure shows the PORP placement at an angle, 20–30°, to the piston-like motion of the stapes (dotted lines). (TB #25)

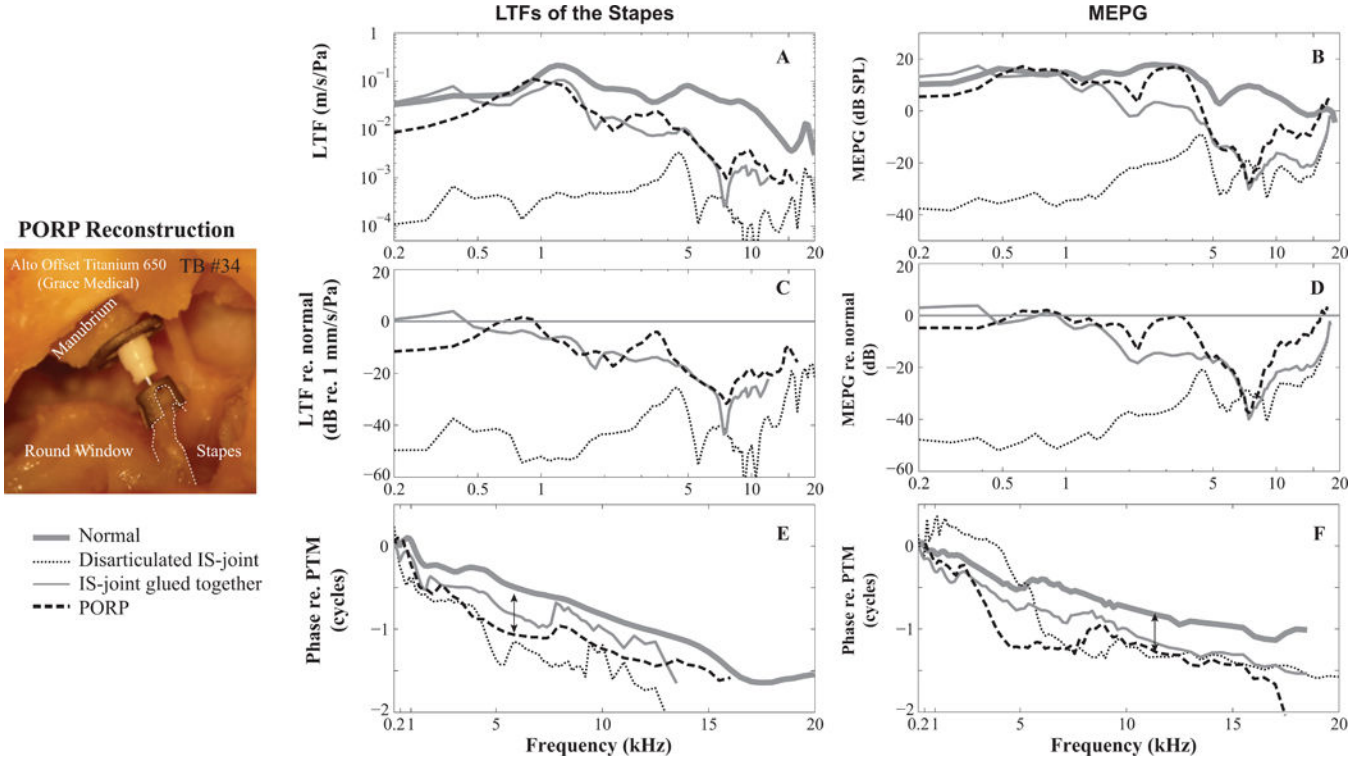

Figure 4. Stapes LTFs and MEPGs under normal and pathological conditions

A and B: amplitude of the stapes LTFs and MEPGs; (C and D) Variation of the stapes LTFs and MEPGs from normal condition; (E and F) phase of stapes LTFs and MEPGs. Double headed arrows indicate 0.5-cycle phase shifts (see Figure 5). Figure legend at the bottom left. Micrograph panel at left side of figure shows the PORP placement along the piston-like motion direction of the stapes (dotted lines). (TB #34)

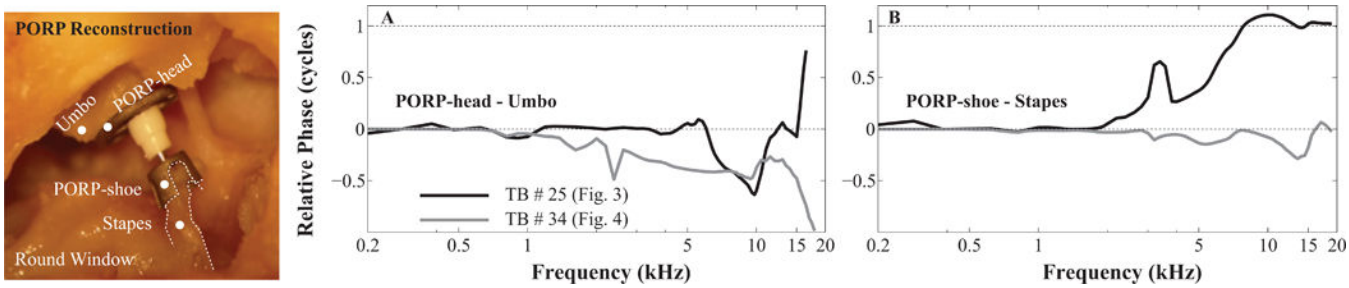

Fig. 5. Evaluation of PORP motion relative to the connecting ME structures

A: phase differrence of the umbo and PORP-head; B: phase difference of the stapes and PORP-shoe. Black and gray lines stand for TB #25 and #34, respectively.

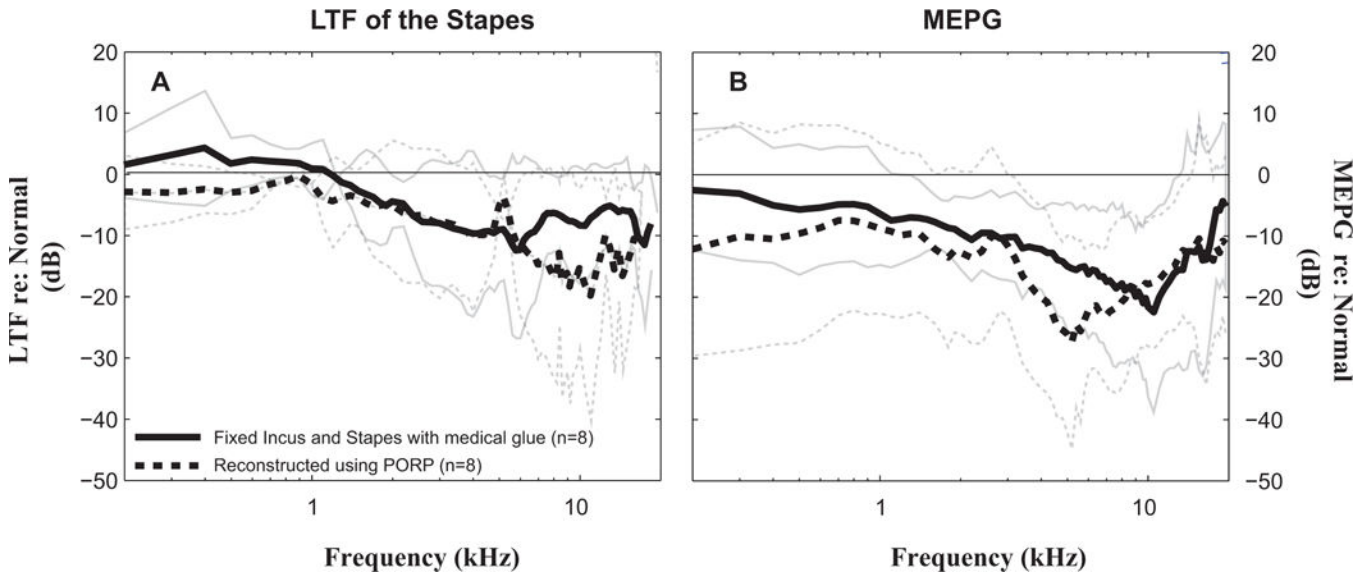

Figure 6. Outcomes of middle-ear repair or reconstruction

A: Mean differences ± 1 standard deviation of stapes LTFs from the normal-control condition. (averaged across eight temporal bones); B: Mean differences ± 1 standard deviation of MEPG from the normal-control condition. (averaged across eight temporal bones). Solid and dashed lines represent glued and PORP conditions, respectively.